Comparison of Different Loop Bioreactors Based on Hydrodynamic Characteristics, Mass Transfer, Energy Consumption and Biomass Production from Natural Gas

Yazdian, Fatemeh; Shojaosadati, Seyed Abbas*+; Nosrati, Mohsen; Vasheghani-Farahani, Ebrahim

Department of Biotechnology, Faculty of Chemical Engineering, Tarbiat Modares University
P.O. Box 14115-143 Tehran, I.R. IRAN

Mehrnia, Mohammad Reza

School of Chemical Engineering, College of Engineering, University of Tehran, Tehran, I.R. IRAN

ABSTRACT: *The performance of a forced-liquid Vertical Tubular Loop Bioreactor (VTLB), a forced-liquid Horizontal Tubular Loop Bioreactor (HTLB) and a gas-induced External Airlift Loop Bioreactor (EALB) were compared for production of biomass from natural gas. Hydrodynamic characteristics and mass transfer coefficients were determined as functions of design parameters, physical properties of gases as well as operational parameters. Moreover, energy consumption for different gas and liquid flow rates was studied. In the EALB, kinematic viscosity (υ_g) showed its significant role on mixing time, gas hold-up and k_La and the diffusion coefficient of gas in water (D_g) had a remarkable effect on k_La. It was observed from experimental results that the performance of the VTLB was the best for biomass production. Furthermore, the volumetric mass transfer coefficients for air and methane were determined at different geometrical and operational factors. New correlations for mixing time, gas hold-up and k_La were obtained and expressed separately. Also, the different ratios of methane and air were measured and compared for optimum growth in the VTLB, HTLB and EALB.*

KEY WORDS: *Forced-liquid vertical tubular loop bioreactor, Forced-liquid horizontal tubular loop bioreactor, Gas-induced airlift loop bioreactor, Hydrodynamic, Mass transfer, Energy consumption.*

INTRODUCTION

In chemical industries, the production costs are mainly influenced by chemical and other running costs. The same hold true for the manufacture of biotechnological costs [1]. In the case of production with

* To whom correspondence should be addressed.
+ E-mail: shoja_sa@modares.ac.ir
1021-9986/10/4/37 20/$/4.00

aerobic microorganism, the key factors are the costs of chemicals and energy. Therefore, for the selection of suitable bioreactors, their specific performance (mass transfer efficiency and energy consumption) are significant.

Loop bioreactors are characterized by a definitely directed circulation flow which can be driven in fluid or fluidized systems by propeller or jet drive and mainly in gas-liquid systems by airlift drive or liquid pump [2]. They are especially appropriate for fluid systems requiring high dispersion priority. On the other hand, their simple constructions and operation result in low investment and operational costs [3]. Also, loop bioreactors have shown an acceptable performance for the production of biomass from natural gas due to their unique hydrodynamic characteristics [2-5]. However, their optimal design and operation for large scale production plants still require vast research. A gas-induced airlift loop bioreactor is a device in which a region of gassed liquid is connected to a region of ungassed liquid; so that the difference in hydrostatic pressure between the two regions results in circulation of the liquid [6]. The forced-liquid bioreactors are constructed with an outlook to provide low-compressed gas injection, long residence time, low energy consumption, simple design and good separation of gases and liquid. Moreover, turbulence generated by forced circulation reduces bubble size and prevents heterogeneous flow from occurring at the maximum aeration velocity. Without liquid circulation, higher aeration rates increase bubble size, cause churn turbulent flow and lead to reduce mass transfer efficiency [6,7].

Methanotrophic bacteria are a group of aerobic bacteria that can use methane as their source of carbon and energy [8]. The processed biomass extracted from these species of microorganisms could be utilized as a source of potential food [7-10]. Past investigations on methane fermentation are mostly devoted to the metabolic pathways of methane oxidation and the taxonomy and physiology of methane-utilizing organisms [11-13]. Although loop bioreactors are employed in fermentation of other carbon sources, and some technical data are available in this regard [4,14-16], data have not been provided and compared for significant factors such as design and operational parameters for methane fermentation in loop bioreactors.

In this research, the comparison of the VTLB, HTLB and EALB and their performance are studied based on hydrodynamic characteristics (i.e., mixing time and gas hold-up), mass transfer efficiency (E_m), energy consumption as well as biomass production. Mixing time, gas hold-up, and k_La are all correlated as responses of operational and design parameters as well as gas phase properties. Superficial gas and liquid velocity selected as the most common operational factors whereas riser (discharge) to downcomer (suction) cross sectional area ratio (A_r/A_d), horizontal length to diameter ratio (L/D), vertical length to diameter ratio (H/D) and volume of gas-liquid separator (S) are defined as design parameters. Furthermore, in the EALB, kinematic viscosity (υ_g), including viscosity (μ) and density (ρ), and diffusion coefficient of dissolved gas (D_g) are chosen and considered as the parameters for gas properties, too. Since the flow in VTLB and HTLB is because of the force of pumps impose on the liquid, the investigation of the effects of gas properties will be restricted and could not be addressed to achieve into trustable results. Therefore, the influence of gas properties such as gas kinematic viscosity and gas diffusion coefficients were studied only in the EALB.

EXPERIMENTAL SECTION

Microorganism and growth medium

The microorganism (*Methylomonas* spp.) used in this work was isolated from an oil field in Iran during the research work in our previous investigation on a bubble column bioreactor [9]. The growth medium was a carbonless salt broth medium named as Methane Salt Broth (MSB) which has been optimized by *Yazdian et al.* [9].

Gas mixture

Five streams of mixed gases were used for evaluation of biomass production. Inlet gas flow rates of air and methane were adjusted so that it would provide mixtures from 25 vol% to 75 vol% air (five streams with ten vol% interval). When oxygen is present in a gas (such as air), the proportion of methane to air is normally in the range of 5 to 15 volumes of methane to 95 to 85 volumes of air to form a flammable mixture [17] however, since gases were spareged right after mixing and passed for single time through the liquid phase, all experiments were carried out safely. Moreover, in the rest of experiments

Table 1: Characteristics of the loop bioreactors used for mixing studies.

Characteristics	Unit	Reactor type		
		EALB	VTLB	HTLB
D	m	-	-	0.03
D_d	m	0.03	0.03	-
D_r	m	0.03,0.06,0.09	0.03	-
D_s	m	0.11,0.18,0.25	0.11,0.18	0.11,0.18
A_r/A_d	-	1.00,4.00,9.00	1.00	1.00
h_s	m	0.10	0.10	0.10
H/D	-	-	45,67	-
L/D	-	-	-	37,54
$S=V_{su}/V_{di}$	-	0.61,1.65,3.11	0.61,1.65	0.61,1.65
N	-	6	6	6
D_0	mm	0.10	0.10	0.10
LP	-	-	MP	M

(for pure gases that are not combustible) air and methane were used individually for the experiments.

Bioreactor

Three experimental loop bioreactors (laboratory scale made of glass), which operated with air and water, were used. The EALB and the VTLB configurations consisted of two vertical columns connected at the top (separator) and the base by horizontal piping. In addition there is a liquid pump just the bottom of the downcomer in the VTLB. The HTLB consists of two long horizontal parts, short vertical downstream and upstream tubes, a top part which is placed right above the upper end of the downstream and a U-shape bend. The geometrical characteristics of the devices are given in Table 1 and illustrated in Fig. 1. The air was distributed by a perforated tube through a gas pump in different zones of the loop bioreactors. The difference in hydrostatic pressure between the two regions in the EALB results in circulation of the liquid. However, in the VTLB and HTLB, the liquid medium was circulated by a liquid magnetic pump. All experiments were carried out at 30 (±0.5) °C. This was done by a Temperature Loop Controller (TLC) placed inside the dissolved methane detector and connected to an electrical heater positioned at the top of the loop bioreactors. Also, a cooling system was used for removing the microbial heat produced during the fermentation process.

Measurements

Dissolved methane

A dissolved methane sensor based on silicone tube was implemented to determine methane concentration during methane fermentation. The silicone tube diameter, silicone tube length and helium flow rate (as the carrier gas) were 0.25 cm (inner diameter) and 0.35 cm (outer diameter), 0.1 m and 50 mL/min, respectively. A continuous stream of helium was directed through the tubing, sweeping out the dissolved methane which diffused through the walls of the tubing from the fermentation broth. The probe of the sensor was made of silicone rubber tubing (NO 02502; Detakta Company). A semi-conductor methane gas sensor (Figaro TGS 2611)-which is highly sensitive and selective to methane gas-was used to measure the dissolved methane continuously [61].

Mixing time

Mixing time (t_m) was determined using tracer response techniques when air was introduced. This technique is based on the fact that if a pulse of tracer (a dye) is injected to the flow, a decaying sinusoidal type of response is detected at the downstream of the injection point [3,18]. Tracer (0.5 ml, Brilliant Blue G, λ=595 nm) was injected to the gas-liquid separating section. Values of optical density were recorded in a spectrophotometer

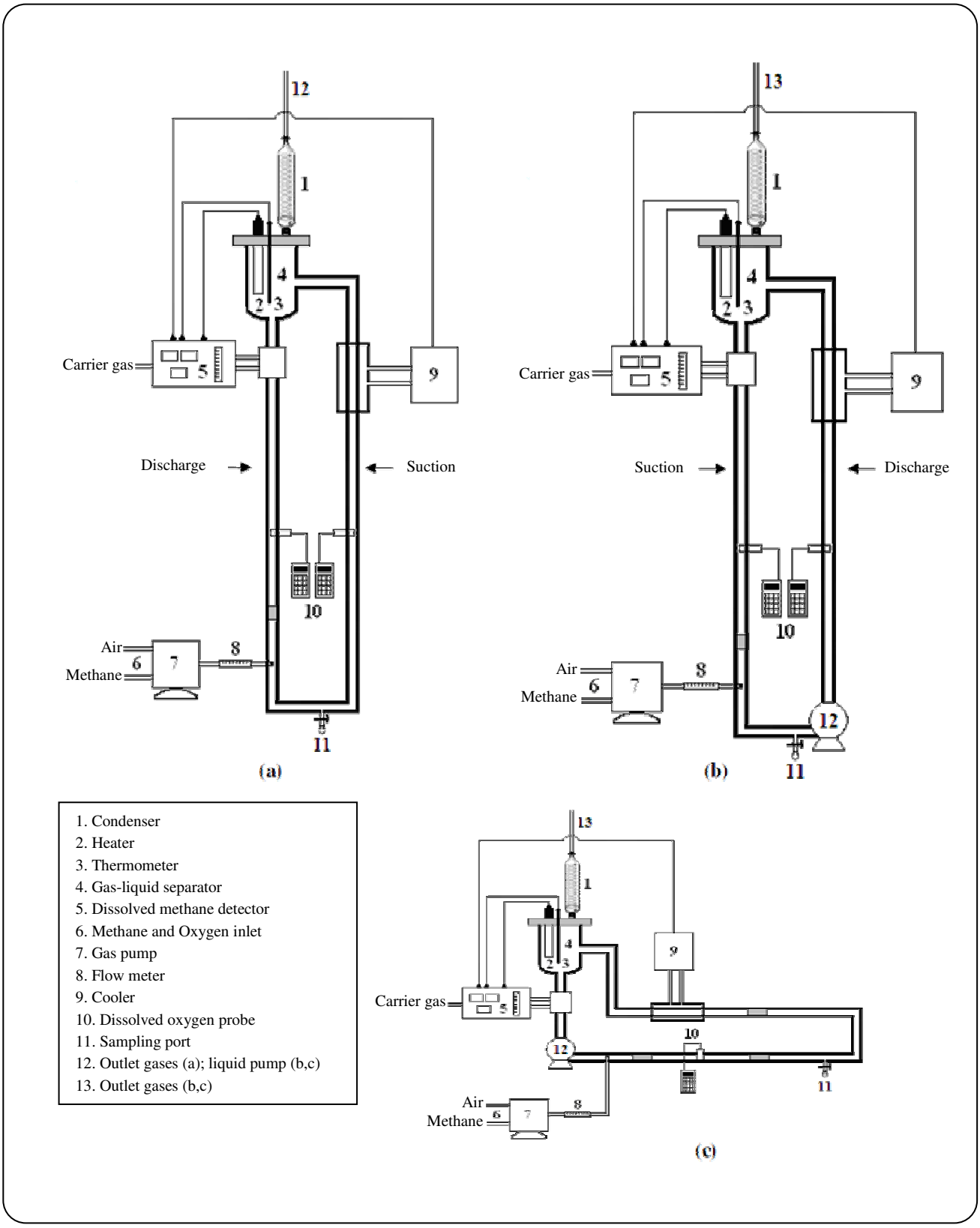

Fig. 1: A schematic diagram of loop bioreactors (a: gas-induced EALB; b: forced–liquid VTLB; c: forced–liquid HTLB).

(VARIAN CARRY 50 CONC, Australia) until the response of the pulse was completely damped (each experiment was carried out in triplicate). Thereafter, mixing time was determined after changing H/D, L/D, separator volume, U_{sG} and U_{sL} and gas composition (only in EALB).

Gas hold-up and mass transfer coefficients (k_La_{O2} and k_La_{CH4})

In addition to methane detector, one probe of dissolved oxygen (DO; with response time of four seconds for 63 % saturation) was placed within the vertical part. Overall gas hold-up (ε), k_La_{O2} and k_La_{CH4} were determined by the eminent methods of volume expansion and dynamic gassing-out measurement respectively [6,19]. For k_La_{O2} measurement, dissolved oxygen was first removed from the bioreactor by sparging with nitrogen until the dissolved oxygen concentration fell down to nearly zero. The nitrogen flow was then stopped and bubbles were allowed to separate from the liquid. When the bioreactor had reached a hydrodynamic steady state, the increase in DO was measured with time until the fluid became nearly saturated with oxygen. The mass balance of DO in the bioreactor, then gives Eq. (1) [6]:

$$\frac{dC_L}{dt} d_L a\left(C^* - C_L\right) \quad (1)$$

where C_L is the DO concentration, C* is saturated oxygen concentration and t is time. Concentration of dissolved methane was measured by methane detector and its volumetric coefficient was determined by a simple method presented previously [20,21]. Also, k_La (oxygen and methane) and ε were determined after changing H/D, L/D, separator volume, U_{sL} and U_{sG} and gas composition (only in EALB) as well.

Power input

The total power input to a two-phase reactor (e_T) could be determined from contribution of each phase in energy consumption. For forced-liquid tubular reactors, four sources of power delivered to the reactor were considered [6,22]: (1) isothermal expansion of gas as it moves up the vessel, (2) the kinetic energy of gas sparged, (3) the kinetic energy of the liquid, and (4) energy lost in spargers. Eq. (2) shows the total specific power delivered to the bioreactors.

$$e_T = \left[\frac{Q_m RT}{V_L} \ln\left(1 + \frac{\rho_L g H_L}{P_{ts}}\right)\right] + \left[\frac{\Omega}{2V_L} Q_m M v_0^2\right] + \left[\frac{Q_L}{2V_L} \rho_L U_{sL}^2\right] + \frac{\Delta P_s Q_L}{V_L} \quad (2)$$

The first, second, third and fourth terms on the right–hand side of Eq. (2) represented power input due to isothermal expansion of the gas, the kinetic energy of the injected gas, the kinetic energy of the liquid entering the reactor and the energy loss in the sparger or static mixer. The efficiency factor Ω was taken to be 1 [6].

RESULTS AND DISCUSSION

Comparison of loop bioreactors based on mixing performance

The mixing characteristics of loop bioreactors of different configurations can be compared by considering the time required to achieve a certain degree of mixing (in this study 95 %). The mixing time may also be used as an operation and scale up parameter, its variation being dependent on the operational and geometrical conditions. To predict or compare the mixing times in the loop bioreactors which were being designed or made, as a function of the operating and geometry variables and gas phase properties, the specific mixing time, denoted as the mixing time per unit liquid volume (t_m/V), is usually used. These specific mixing time concept has also been used previously by *Rousseau & Bu'Lock* [23], *Popovic & Robinson* [24] and *Gavrilescu & Tudose Radu* [25]. We determine the mixing time with the same method and define a geometrical parameter such as S to interpret the effect of the volume of the separator, H/D to illustrate the influence of VTLB height and L/D to present the impression of HTLB length. H/D and L/D obtain two values (see Table 1).

Like all the authors which investigated the influence of the gas velocity, the same results have been observed in this study. In all devices investigated, the mixing time decreases with an increasing aeration rate. In the EALB, two regimes of mixing time were observed. At low gas velocities, mixing time decreased sharply, while at higher velocities mixing time was almost constant (Fig. 2). Especially in laboratory systems, the mixing time becomes less efficient at higher gas velocities. These values of gas velocity correspond to the transition from the circulating to the turbulent regime. In the EALB, Fig. 2 shows when

kinematic viscosity (υ_g) increased from 19.04×10^{-6} Pa.s (for oxygen) to 27.54×10^{-6} Pa.s (for methane), mixing time increased as well (i.e., mixing time changes directly). Kinematic viscosity showed its role significantly on mixing time when different gases (oxygen, methane and their mixtures) were used.

Mixing time decreased with increasing values of both gas and liquid flow rates in the VTLB and HTLB, too. Our experiments showed that there are two zones of the dependency of mixing time on gas velocity (Figs. 3 and 4). For different values of gas velocity (in this study), mixing time was sensitive at low liquid velocities; while at higher liquid velocities, mixing time was less affected by high values of aeration rates. In the VTLB, at low gas velocities mixing time was highly sensitive to different amounts of liquid circulation rates. However, in the HTLB, mixing time was sensitive to low gas velocity especially at low liquid flow rates.

Figs. 2 to 4 show that when the amount of A_r/A_d, L/D and H/D decreased from 4 to 1; 54 to 37 and 67 to 45, respectively, the mixing time decreased, too. These are expectable and also have been shown by many investigators that observed a decrease in the mixing time with decrease of known geometrical parameters such as A_r/A_d, L/D and H/D ratio [26-29]. Also, no discernible effect of the separator volumes on mixing time was observed (0.61 and 1.65 for S). However, in the EALB, separator volume showed its role considerably in compare to the VTLB and HTLB. It is necessary to find the minimum critical value of S for optimum operation of the mentioned loop bioreactors in further studies. The effect of design factors on mixing time in the investigated loop bioreactors (particularly in the EALB) can therefore be attributed mainly to the effect of design parameters (e.g., A_r/A_d) on the recirculation of liquid velocity, which proves to be the physical parameter which most strongly affects the recirculation rates in the none-forced liquid loop bioreactors. Therefore, the mixing time can be considered as a measure of the macro-scale mixing by convective mechanisms [6].

Based on our experimental results, some new correlations for normalized mixing time (t_m/V) were presented in Eqs. (3) to (5) [30].

$$\frac{t_m}{V}=1.11U_{sG}^{-0.70}\times\left(1+\frac{A_r}{A_d}\right)^{0.46}\times(1+S)^{-0.42}\times\left(\frac{\upsilon_g}{\upsilon_{N_2}}\right)^{0.43} \quad (3)$$

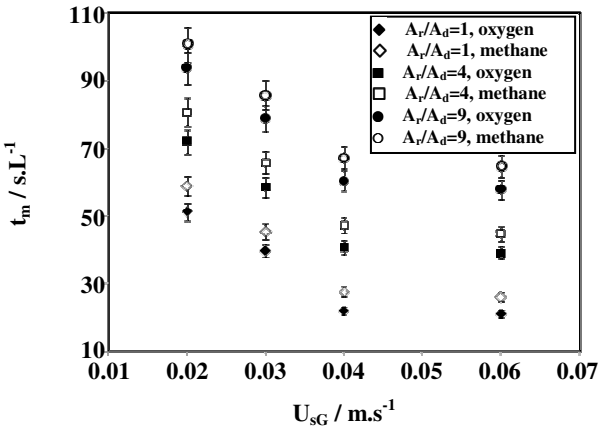

Fig. 2: Normalized mixing time versus superficial gas velocity in the EALB (the error-bars-shapes given in Fig. 2 are related to the effects made by the gas separator size).

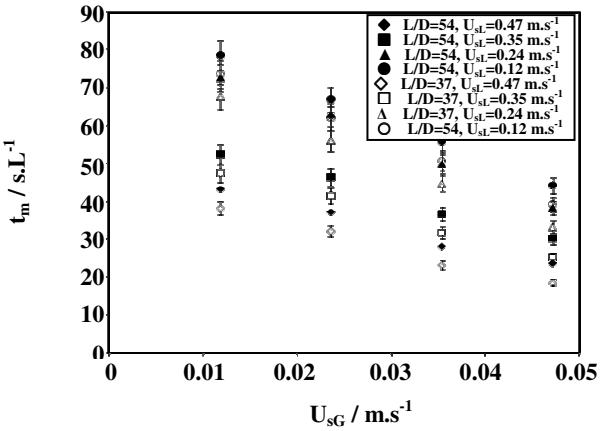

Fig. 3: Normalized mixing time versus superficial oxygen velocity in the HTLB (the error-bars-shapes given in Fig. 3 are related to the effects made by the gas separator size).

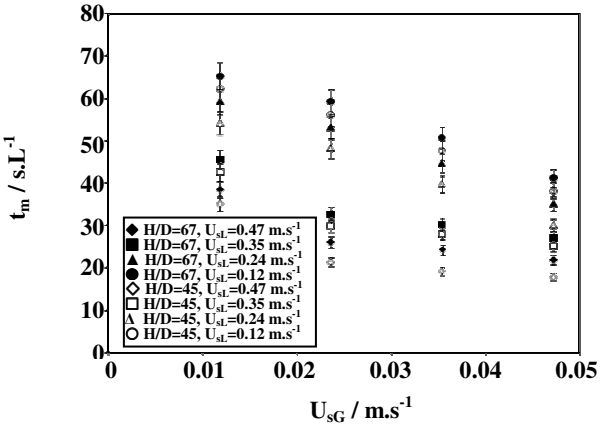

Fig. 4: Normalized mixing time versus superficial gas velocity in the VTLB (the error-bars-shapes given in Fig. 4 are related to the effects made by the gas separator size).

In addition to operational and design parameters, the effect of physical properties of the gases were combined and considered in Eq. (3). We entered the kinematic viscosity ($\upsilon_g=\mu/\rho$) of the gas as a physical property which causes the changes in the mixing time, circulation time, gas hold-up, and gas volumetric mass transfer coefficient (k_La). The term of normalized gas density (ρ_g/ρ_l) is another interesting alternative for allocating the effect of gas type on hydrodynamic and mass transfer characteristics. However, since the density of the gases is very small, it provides a very small value in the correlation too, and naturally causes constant coefficient to be tremendously increased. The physical property of υ_g was normalized by its dividing by the property of an inert gas such as nitrogen (υ_g/υ_{N2}). Since we considered the effect of the type of the gas, our correlation provides a new contribution compared with the other correlations [23,29]. The range of applicability for Eq. (3) is 0.02 to 0.06 $m.s^{-1}$ for superficial gas velocity. The value of A_r/A_d is 1 to 9. Also, the ratio of separator volume to downcomer volume is 0.61 to 3.11. Moreover, the υ_g/υ_{N2} value is 1.12 to 1.62. Values estimated with Eq. (3) agreed with the experimentally measured data with less than 14% error.

Depending on the gas velocity range, the exponent for U_{sG} has the values from -0.075 to -0.60 [25,31,32]. The exponent of U_{sG} in our correlation is however next to the range previously reported by other researchers. The influence of A_r/A_d on hydrodynamic characteristics in external loop bioreactors was investigated experimentally by *Bello et al.* [33]. Their results showed that mixing time increased with the increase of this ratio (A_r/A_d), with an exponent of 0.26. *Joshi et al.* [34] theoretically predicted the value of 0.37 for the exponent. The trend of our results (effect of A_r/A_d on mixing time) is similar to that observed by others. *Weiland* [26] found that gas-liquid separator volume had strong influence on mixing time. His results presented as t_m versus gas-liquid separator volume gave the slope of -0.39 (the exponent of third variable in Eq. (3) is next to *Weiland*'s).

The dependence of the mixing time on the operational and geometrical velocities expressed by the following equation in the HTLB, too [7]:

$$\frac{t_m}{V}=1.17U_{sG}^{-0.40}\cdot U_{sL}^{-0.56}\cdot\left(\frac{L}{D}\right)^{0.35}\cdot(1+S)^{-0.15} \qquad (4)$$

Eq. (4) determines mixing time by four simple parameters in horizontal loop bioreactors. Its range of applicability is between 0.01-0.05 $m.s^{-1}$ and 0.12-0.47 $m.s^{-1}$ for superficial gas and liquid velocities respectively. L/D is between 37-54. Also, S is 0.61 to 1.65. Eq. (4) correlated 90% of the data with less than 20% error. This maximum deviation only states in which ranges the measured and calculated data cover each other. The unit of normalized mixing time is time to volume (for example s/L).

On the basis of our experimental results in the VTLB, a new correlation for normalized mixing time (t_m/V) is presented by Eq. (5) [35]:

$$\frac{t_m}{V}=1.37U_{sG}^{-0.34}\cdot U_{sL}^{-0.59}\cdot\left(\frac{H}{D}\right)^{0.28}\cdot(1+S)^{-0.09} \qquad (5)$$

Eq. (5) determines mixing time by four simple parameters in forced-liquid vertical loop bioreactors. Estimated values by Eq. (5) agreed with the experimentally measured data with less than 18% error. The range of applicability for eq 5 is 0.01 to 0.06 $m.s^{-1}$ for superficial gas velocity. The value of H/D is 45 to 67. Also, the ratio of separator volume to discharge side volume is 0.61 to 1.65. Moreover, the liquid flow rate is 0.1 to 0.6 $m.s^{-1}$.

The exponent of U_{sG} in our correlation is next to the range reported by *Yazdian et al.* [7] for forced–liquid loop bioreactors. Dependence of mixing time on gas and liquid flow rates was studied in forced-liquid loop bioreactors by *Chisti et al.* [36], *Fadavi & Chisti* [37] and *Fadavi & Chisti* [38] as well. They concluded that mixing time decreased with increasing values of both gas and liquid flow rates (both gas and liquid velocities contributed to promoting mixing in the bioreactor). Moreover, the effect of liquid flow rate on mixing time has the same consequence in comparison with *Yazdian*'s results (the exponent of U_{sL} are 0.56 and 0.59). The influence of design factor on hydrodynamic characteristics in forced-liquid loop bioreactors was investigated experimentally by *Yazdian et al.* [7], too. Their results showed that mixing time increased with the increase of geometry parameters, with an exponent of 0.35. The trend of our results (effect of H/D on mixing time) is similar to that observed by others [26-29]. *Yazdian et al.* [7] found that gas-liquid separator volume had no big influence on mixing time. Their results presented as t_m versus gas-liquid separator volume gave the slope of -0.15

Table 2: Comparison of mixing time correlations for different loop bioreactors.

characteristics	correlation	R^2
gas–induced EALB	$\frac{t_m}{V} = 1.11 U_{sG}^{-0.70} \cdot \left(1 + \frac{A_r}{A_d}\right)^{0.46} \cdot (1+S)^{-0.42} \cdot \left(\frac{\upsilon_g}{\upsilon_{N_2}}\right)^{0.43}$	0.92
forced–liquid HTLB	$\frac{t_m}{V} = 1.17 U_{sG}^{-0.40} . U_{sL}^{-0.56} \cdot \left(\frac{L}{D}\right)^{0.35} \cdot (1+S)^{-0.15}$	0.90
forced–liquid VTLB	$\frac{t_m}{V} = 1.37 U_{sG}^{-0.34} . U_{sL}^{-0.59} \cdot \left(\frac{H}{D}\right)^{0.28} \cdot (1+S)^{-0.09}$	0.90

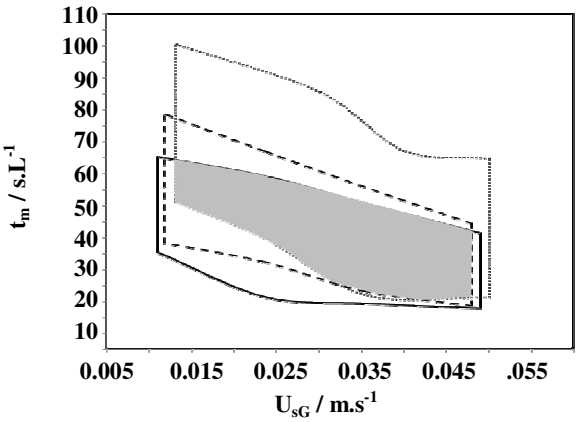

Fig. 5: Comparisons of mixing time versus superficial gas velocity for loop bioreactors: forced–liquid VTLB; ---forced-liquid HTLB; … gas-induced EALB.

(the exponent of fourth variable in Eq. (5) is next to *Yazdian*'s). Furthermore, *Papagianni et al.* [39] used *Verlaan*'s equation to estimate mixing time. The mixing times calculated with the equation of *Verlaan et al.* [40] were very close to those obtained with experimental data in forced–liquid tubular loop bioreactor. They suggested that the relative mixing (t_m/t_c) time is a parameter that can be used with confidence in characterization of mixing in the forced-liquid TLBs.

Fig. 5 illustrates the comparison of mixing time versus superficial gas velocity for different loop bioreactors. The shortest mixing time was achieved in the VTLB. In the HTLB, t_m was more than in the forced-liquid VTLB. However, mixing times in the HTLB and VTLB were less than in the EALB; because of the increased liquid velocity in the forced–liquid loop bioreactors. Therefore, the experimental results showed that the greatest mixing times were obtained in the EALB. According to experimental outcomes, the forced–liquid circulation (in the VTLB and HTLB) led to a shortening in the mixing time about 30% compared to the EALB. This behavior indicated that mixing processes was predominately controlled by the macro-circulation of the liquid phase within the loops and to a lesser extent by the axial dispersion due to ascending bubbles [25]. Due to the presented data, a region (it was shown in gray color in Fig. 5) that was independent on bioreactor type was explored that occurred in gas superficial velocity that ranged between 0.015 m.s^{-1} to 0.047 m.s^{-1}. In that zone, mixing time was not reliant on bioreactor variety and changed with variation of operational and design parameters, only. The comparison of experimental results for mentioned loop bioreactors (based on correlations) are compared in Table 2.

Comparison of loop bioreactors based on gas hold-up

Gas hold-up versus superficial gas velocity in the EALB for different gases and A_r/A_d are illustrated in Fig. 6. It can be seen when kinematic viscosity increased from 19.04×10^{-6} Pa.s (for oxygen) to 27.54×10^{-6} Pa.s (for methane), gas hold–up decreased, too. Gas hold-up for different gases (oxygen, methane, and their mixtures) changed with υ_g indirectly; whereas it increased directly as gas velocity enhanced. In the mentioned loop bioreactors, gas hold-up increased as oxygen velocity increased. However, the dependence of ε on superficial gas velocity became slightly weak at high gas flow rates (more than 0.04 m.s^{-1}). However, in the HTLB and VTLB, at any constant value of the oxygen velocity, the overall gas hold–up increased by increasing the liquid velocity (Figs. 7 to 9). Increasing liquid flow rate reduced bubble size of the gas stream and consequently increased hold-up. It is, however, expectable; because turbulent liquid movements create eddies those hit the bubbles sharply and make them smaller and avoid their easy escape from the top of the reactor. A significant enhancement in gas hold-up occurred at the liquid velocity of 0.47 m.s^{-1} which resulted in a gas hold-up of

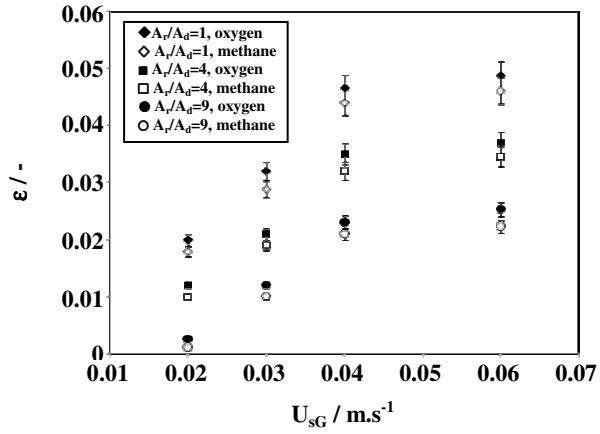

Fig. 6: Gas hold–up versus superficial air velocity in the EALB (the error-bars-shapes given in Fig. 6 are related to the effects made by the gas separator size).

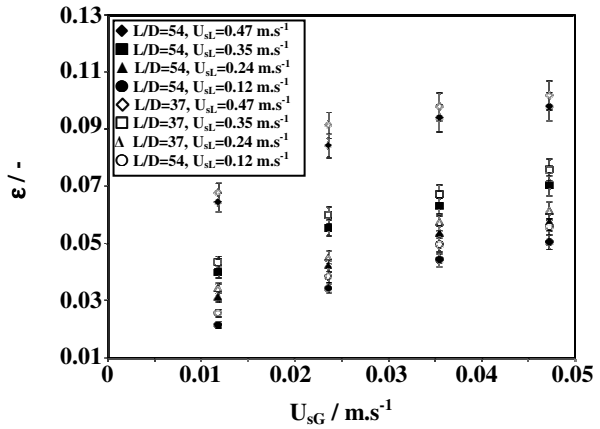

Fig. 7: Gas hold–up versus superficial air velocity in the HTLB (the error-bars-shapes given in Fig. 7 are related to the effects made by the gas separator size).

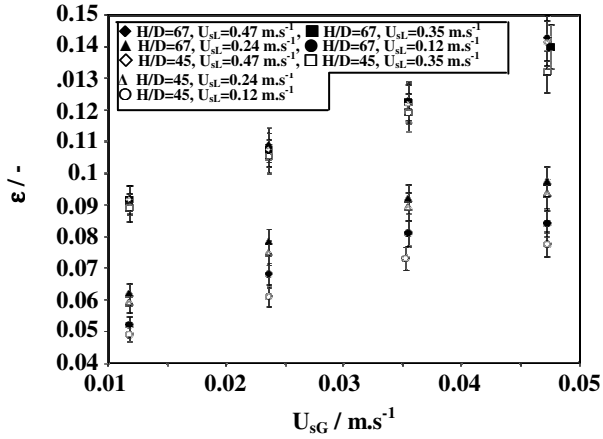

Fig. 8: Gas hold–up versus superficial air velocity in the suction side of the VTLB (the error-bars-shapes given in Fig. 8 are related to the effects made by the gas separator size).

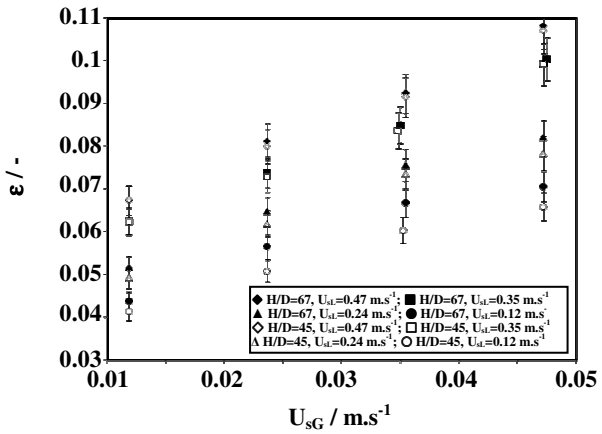

Fig. 9: Gas hold-up versus superficial air velocity in the discharge side of the VTLB (the error-bars-shapes given in Fig. 9 are related to the effects made by the gas separator size).

0.1 (in the HTLB). In the suction side of the VTLB, as could be seen in Fig. 8, the amount of gas hold-up increased significantly even at low liquid velocities. Increasing of liquid flow rate reduced bubble size of the gas stream and consequently increased hold-up (to 0.14) only up to a liquid velocity of 0.35 m.s^{-1}. A further increase in liquid velocity to 0.47 m.s^{-1} hardly had any effect on the suction gas hold-up. The bubble columns and airlift reactors do not generally exceed an overall gas hold–up value of 0.1 in air-water systems [6,36-38]. In contrast, the forced circulation operation at a relatively low liquid velocity of 0.24 m.s^{-1} attained a gas hold-up (in suction part of the VTLB) around 0.10. Here, bubble flow regime persisted to a gas hold-up achieve 0.14 during the forced circulation operation.

The discharge gas hold-up changed with the gas and liquid velocities as shown in Fig. 9 as well. During operation at lower values of liquid injection rate, little gas bubbles were dragged into the discharge zone. Consequently, there was hardly any gas bubble to be held in the discharge part under these conditions (Fig. 9). A significant number of bubbles began to be dragged into the discharge once the velocity of gas in the suction part exceeded 0.035 m.s^{-1} in low liquid flow rates. Although an increase of forced flow liquid velocity from 0.35 m.s^{-1} to 0.47 m.s^{-1} did not increase the suction gas hold–up (Fig. 8), it significantly enhanced the discharge gas hold-up as more bubbles were dragged in the discharge zone because of a high flow rate of liquid.

The influence of the geometrical parameter (A_r/A_d) on ε is clearly sketched in Fig. 6 (in the EALB). Decrease in A_r/A_d ratio led to an increase in ε. The increase in gas hold-up with decreasing A_r/A_d, resulted from reduced liquid circulation due to the increasing resistance of the liquid circulation path. Some investigators proposed their empirical correlations for gas hold-up with U_{sG} and A_r/A_d [23,41,42]. But in their correlations the effect of separator volume has not been studied. *Kawase et al.* [43] presented his non-Newtonian correlation for gas hold-up with the geometrical parameter A_r/A_d, too. In the HTLB, a decrease in L/D ratio led to an increase in ε. The increase of gas hold-up with decreasing L/D ratio resulted from generation of small bubbles due to increase of the bubble velocity. In the VTLB, increase in H/D ratio led to a slight increase in ε. Increasing gas hold-up as a direct result of H/D ratio, enhances the hydrostatic pressure and also generation of small bubbles due to the increase of bubble velocity.

We presented our correlation for gas hold−up in riser (discharge) side of the EALB for the experimented gases (oxygen, methane, and gas mixtures) by Eq. (6) [30]:

$$\varepsilon_{di} = 13.19 U_{sG}^{1.43} \cdot \left(1+\frac{A_r}{A_d}\right)^{-0.62} \cdot (1+S)^{-0.58} \cdot \left(\frac{\upsilon_g}{\upsilon_{N_2}}\right)^{-0.52} \quad (6)$$

As is obvious, we preserved the dependency of our correlation to geometrical characteristic (A_r/A_d), separator volume, superficial gas velocity, and gas properties again. The resulting correlation is simple and hence usable for fermentation. Its range of applicability is 0.02 to 0.06 $m.s^{-1}$ for superficial gas velocity. The value of A_r/A_d is 1 to 9. Also, the ratio of separator volume to downcomer volume is 0.61 to 3.11. Moreover, the υ_g/υ_{N2} value is 1.12 to 1.62. Estimated values by Eq. (6) agreed with the experimentally measured data with less than 15% error. The effect of separator volume on gas hold−up could be seen clearly although its affects is less than A_r/A_d. Separator volume showed its role slightly when υ_g and A_r/A_d increased (the error-bars-shapes given in Fig. 6 are related to the effects made by the gas separator size). However, separator volume demonstrated its effect significantly while υg and A_r/A_d decreased.

For all experiments in our research work, gas hold-up was also measured in the downcomer (suction). Gas hold-up measurement revealed that a linear correlation between ε_{di} and ε_{su}. Eq. (7) explains the data fit with 98% agreement for the EALB [30]:

$$\varepsilon_{su} = 0.47\varepsilon_{di} \quad (7)$$

Depending on the gas velocity range, the exponent for U_{sG} has the values from 0.50 to 1.50 [31,44,45]. The exponent of U_{sG} in our correlation is in this range. *Popovic & Robinson* [23] reported an exponent of -1 for the term $(1+A_r/A_d)$ in their work. The exponent of $(1+A_r/A_d)$ in Eq. (6) is however next to *Popovic* and *Robinson*'s. However, the dependency of gas hold−up on $(1+A_r/A_d)$ by *Chisti et al.* [46] is weaker than that in the proposed correlation.

The correlation for oxygen hold−up in the HTLB was presented by Eq. (8) [7]:

$$\varepsilon = 1.1 U_{sG}^{0.41} \cdot U_{sL}^{0.55} \cdot \left(\frac{L}{D}\right)^{-0.18} \cdot (1+S)^{-0.07} \quad (7)$$

Depending on the gas velocity range, the exponent for U_{sG} has the values from 0.50 to 1.50 [31,44,45]. The exponent of U_{sG} in our correlation is in this range. *Popovic & Robinson* [23] reported an exponent of -1 for the term $(1+A_r/A_d)$ in their work. The exponent of $(1+A_r/A_d)$ in Eq. (6) is however next to Popovic and Robinson's. However, the dependency of gas hold-up on $(1+A_r/A_d)$ by *Chisti et al.* [46] is weaker than that in the proposed correlation.

The correlation for oxygen hold-up in the HTLB was presented by Eq. (8) [7]:

$$\varepsilon = 1.1 U_{sG}^{0.41} \cdot U_{sL}^{0.55} \cdot \left(\frac{L}{D}\right)^{0.18} \cdot (1+S)^{-0.07} \quad (8)$$

As is obvious, this correlation again depends on geometrical characteristic (L/D and S), superficial gas and liquid velocity. The range of applicability of gas hold−up is between 0.01-0.05 $m.s^{-1}$ and 0.12-0.47 $m.s^{-1}$ for superficial gas and liquid velocities respectively. L/D is between 37-54. Also, S is 0.61 to 1.65. Gas hold-up is dimensionless. Eq. (8) correlated 93% of the data with less than 20% error. This maximum deviation only states in which ranges the measured and calculated data cover each other. The effect of separator volume on gas hold−up was less; however, it is necessary to find its minimum critical value for optimum operation of the HTLB in other studies (the error-bars-shapes given in Fig. 7 are related to the effects made by the gas separator size).

The correlation for air hold-up in suction and discharge parts of the VTLB was presented by Eqs. 9 and 10, respectively [35]:

$$\varepsilon_{su} = 0.31 U_{sG}^{0.31} \cdot U_{sL}^{0.50} \cdot \left(\frac{H}{D}\right)^{0.13} \cdot (1+S)^{-0.07} \quad (9)$$

$$\varepsilon_{di} = 0.21 U_{sG}^{0.32} \cdot U_{sL}^{0.30} \cdot \left(\frac{H}{D}\right)^{0.13} \cdot (1+S)^{-0.07} \quad (10)$$

These correlations rely on geometrical characteristic (H/D and S) and superficial gas and liquid velocity. Eq. (9) correlated 92% of the data with less than 15% error. Also, estimated values by Eq. (9) agreed with the experimentally measured data with less than ±12% error. Eq. (10) shows that liquid flow rate and gas flow almost have the same effect on gas hold-up in discharge section. The range of applicability for Eqs. 9 and 10 is 0.01 to 0.06 $m.s^{-1}$ for superficial gas velocity. The value of H/D is 45 to 67. Also, the ratio of separator volume to discharge side volume is 0.61 to 1.65. Moreover, the liquid flow rate is 0.1 to 0.6 $m.s^{-1}$. The error-bars-shapes given in Figs. 8 and 9 are related to the effects made by the gas separator size.

Depending on the gas velocity range, the exponent for U_{sG} has the values from 0.3 to 0.9 in forced-liquid loop bioreactors [7,36-38]. *Fadavi & Chisti* [38] showed an exponent of 0.9 for this variable. The exponent of U_{sG} in our correlation is in the mentioned range. *Chisti et al.* [36], *Fadavi & Chisti* [37], and *Fadavi & Chisti* [38] concluded that mixing time decreased with increasing values of both gas and liquid flow rates in forced-liquid loop bioreactors. Eqs. (8) to (10) show that gas-liquid separator volume had the same influence on gas hold-up like *Yazdian*'s results (the exponent of fourth variable in mentioned equations are 0.07) [7].

Fig. 10 illustrates the comparison of gas hold-up versus superficial gas velocity for different loop bioreactors. The shortest gas hold-up was achieved in the EALB. In the VTLB, gas hold-up was more than in the forced–liquid HTLB. However, gas hold-ups in the HTLB and VTLB were more than in the EALB obviously; because of the increased liquid velocity in the forced-liquid loop bioreactors. Therefore, the experimental results showed that the biggest gas hold-ups were obtained noticeably in the VTLB. According to experimental outcomes, the forced-liquid circulation

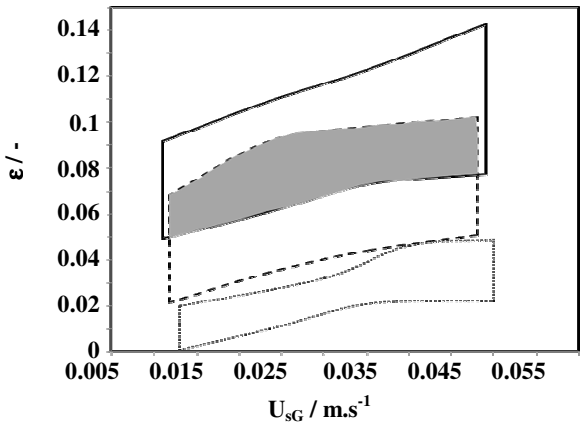

Fig. 10. Comparisons of gas hold–up versus superficial gas velocity for loop bioreactors: forced–liquid VTLB; --- forced-liquid HTLB; … gas-induced EALB.

(in the VTLB and HTLB) led to an extension in the gas hold-up about 66% compared to the EALB. Due to the presented data, a region (it was shown in gray color in Fig. 10) that was independent on bioreactor type (HTLB and VTLB) was explored that occurred in superficial gas velocity that ranged between 0.015 $m.s^{-1}$ to 0.047 $m.s^{-1}$. In that zone, gas hold-up was not reliant on bioreactor variety (HTLB and VTLB) and changed with variation of operational and design parameters, only. The comparison of experimental results for mentioned loop bioreactors (based on correlations) are compared in Table 3 as well.

Comparison of loop bioreactors based on mass transfer coefficients

Fig. 11 shows the experimental gas volumetric liquid mass transfer coefficients (k_La) in discharge side of the EALB versus superficial gas velocity for different gases and A_r/A_d. kinematic viscosity (υ_g) showed its significant role on k_La when different gases (oxygen, methane and their mixtures) were used. When kinematic viscosity increased from 19.04×10^{-6} Pa.s (for oxygen) to 27.54×10^{-6} Pa.s (for methane), k_La reduced. Moreover, k_La increased when diffusion coefficient increased from 1.8×10^{-9} m^2/s (for methane) to 2.51×10^{-9} m^2/s (for oxygen). It was revealed that diffusion coefficient of gas in water (D_g) has remarkable effect on k_La. In addition, changes in the amount of A_r/A_d in Fig. 11 resulted in same effects as shown in Fig. 6 for gas hold-up (because the hold-up is the main factor that influences the gas-liquid interfacial area). It was shown that separator volume had a more effective contribution on

Tahle 3: Comparison of gas hold-up correlations for different loop bioreactors.

characteristics	correlation	R^2
gas−induced EALB	$\varepsilon_{di} = 13.19U_{sG}^{1.43} \cdot \left(1+\frac{A_r}{A_d}\right)^{-0.62} \cdot (1+S)^{-0.58} \cdot \left(\frac{\upsilon_g}{\upsilon_{N_2}}\right)^{-0.52}$	0.90
	$\varepsilon_{su} = 0.47\varepsilon_{di}$	0.98
forced−liquid HTLB	$\varepsilon = 1.1U_{sG}^{0.41} \cdot U_{sL}^{0.55} \cdot \left(\frac{L}{D}\right)^{-0.18} \cdot (1+S)^{-0.07}$	0.93
forced−liquid VTLB	$\varepsilon_{su} = 0.31U_{sG}^{0.31} \cdot U_{sL}^{0.50} \cdot \left(\frac{H}{D}\right)^{0.13} \cdot (1+S)^{-0.07}$	0.92
	$\varepsilon_{di} = 0.21U_{sG}^{0.32} \cdot U_{sL}^{0.30} \cdot \left(\frac{H}{D}\right)^{0.13} \cdot (1+S)^{-0.07}$	0.93

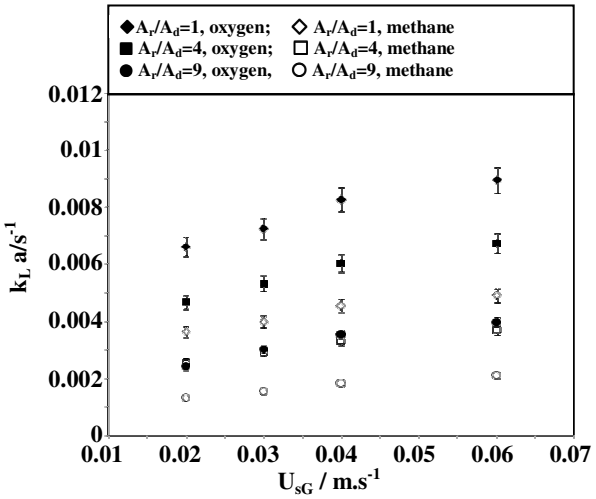

Fig. 11: Mass transfer coefficient versus superficial air velocity in the EALB (the error-bars-shapes given in Fig. 11 are related to the effects made by the gas separator size).

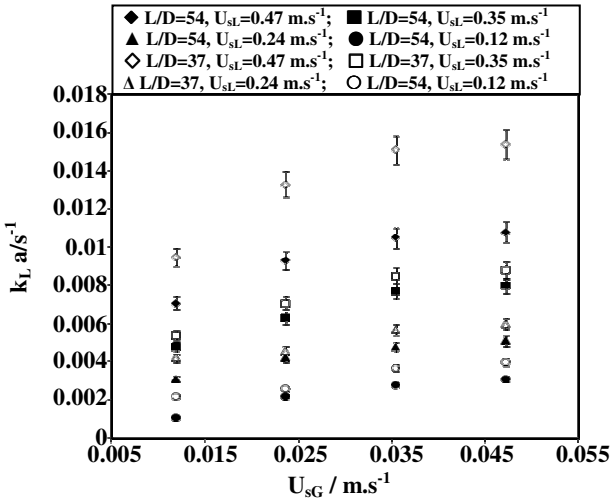

Fig. 12: Mass transfer coefficient versus superficial air velocity in the HTLB (the error-bars-shapes given in Fig. 12 are related to the effects made by the gas separator size).

mass transfer coefficient when υ_g and A_r/A_d decreased (the error-bars-shapes given in Fig. 11 are related to the effects made by the gas separator size). As is predictable, k_La values were enhanced as a result of gas flow rates increase. Figs. 12 to 14 show the experimental oxygen volumetric liquid mass transfer coefficients (k_La_{O2}) in the HTLB and VTLB versus the same parameters shown in Figs. 7 to 9. Similar to gas hold-up, changes in the amount of L/D and H/D resulted in the same effects for k_La. In addition, like the mixing time and gas hold-up, separator volume does not have any more effective contribution on mass transfer coefficient. Predictably, k_La values were enhanced by increasing gas flow rates. The liquid flow mainly influences k_La by affecting the bubble size and gas-liquid interfacial area "a". In the suction of VTLB, increasing liquid flow rate reduced bubble size of the gas stream and, therefore, increased k_La (to 0.034 s^{-1}) only up to a liquid velocity of 0.35 $m.s^{-1}$. A further increase in liquid velocity to 0.47 $m.s^{-1}$ barely had any effect on the suction zone k_La. In spite of mass transfer coefficient in suction zone, the amount of k_La in discharge zone is sensitive to high liquid circulation rate. At high H/D ratios, significant enhancement in k_La occurred in the liquid velocity of 0.47 $m.s^{-1}$ which resulted in a k_La of 0.03 s^{-1}.

Eq. (11) shows the correlation with its corresponded coefficient and powers for the tested gases (oxygen, methane and their mixtures) [30]:

$$(k_La)_{di} = 0.097U_{sG}^{0.46} \cdot \left(1+\frac{A_r}{A_d}\right)^{-0.63} \cdot (1+S)^{-0.61} \cdot \left(\frac{\upsilon_g}{\upsilon_{N_2}}\right)^{-0.91} \cdot \left(\frac{D_g}{D_{N_2}}\right)^{1.12} \qquad (11)$$

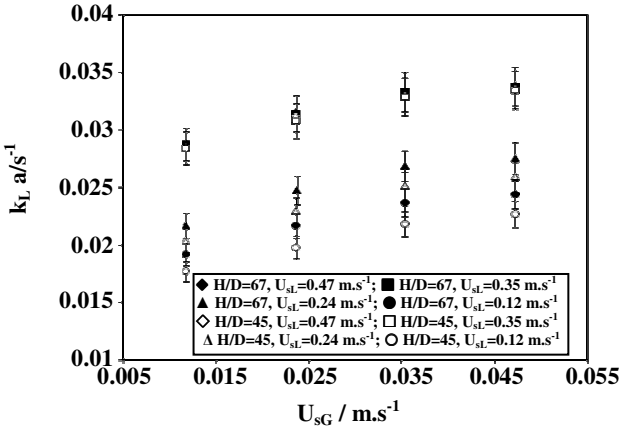

Fig. 13: Mass transfer coefficient versus superficial air velocity in the suction side of the VTLB (the error-bars-shapes given in Fig. 13 are related to the effects made by the gas separator size).

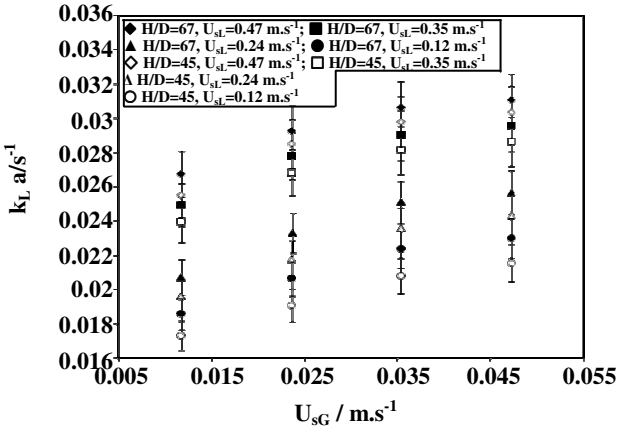

Fig. 14: Mass transfer coefficient versus superficial air velocity in the discharge side of the VTLB (the error-bars-shapes given in Fig. 14 are related to the effects made by the gas separator size).

Compared with Eq. (3) and Eq. (6), for k_La, we allocated one more gas property that affects the mass transfer coefficient of dissolved gas in the liquid. This property is diffusion coefficient of gas in water (D_g). Both physical properties (υ_g and D_g) were normalized by dividing them by the properties of an inert gas such as nitrogen [(D_g/D_{N2}) and (υ_g/υ_{N2})].

Eq. (11) compares experimental values of k_La and its calculated amounts with less than 13% error. Its range of applicability is 0.02 to 0.06 m.s^{-1} for superficial gas velocity. The value of A_r/A_d is 1 to 9. Also, the amount of separator volume to downcomer volume ratio is 0.61 to 3.11. Moreover, the υ_g/υ_{N2} and D_g/D_{N2} values are 1.12 to 1.62 and 0.98 to 1.32, respectively. *Bello et al.* [47] and *Chisti et al.* [48] correlated their theoretical expression for liquid mass transfer coefficient in discharge with familiar and easy-to-work parameters of U_{sG} and A_r/A_d only. By Eq. (11), we extended their correlations by considering the effect of separator volume and physical gas properties on k_La. In spite of the existing literature with liquid phase properties; we investigated the influence of gas type on mass transfer [48-50].

Depending on the gas velocity range the exponent for U_{sG} has the values ranging from 0.4 to 1 [23.47,51,52]. It goes without saying that the exponent of U_{sG} in our correlation is in this range. *Popovic & Robinson* [23] reported an exponent of -0.85 for the term ($1+A_r/A_d$) in their work. The exponent of ($1+A_r/A_d$) in Eq. (11) is next to *Popovic & Robinson*'s. However, the dependency of k_La on ($1+A_r/A_d$) by Bello et al. [47] is significantly more than that in the proposed correlation in this study (Eq. 11).

Despite of the presence of a few studies that experimented superficial gas velocity in downcomer [53] direct correlation of k_La in this section on the basis of gas superficial velocity in riser is not very common. In EALBs, the rising gas bubbles makes liquid flow from down to top; then it returns the flow back from top to down in downcomer section. Since the gas sparger and gas injection devices are located in the riser part and many of bubbles are removed when they reach to the gas-liquid separator, it is not very reasonable to state the downcomer k_La based on superficial gas velocity in riser (U_{sG}). Hence, we only measured the mass transfer coefficients in downcomer and determined its relation with k_La in riser. Eq. (12) explains the data fit with 96% agreement for the fraction of $(k_La)_{su}/(k_La)_{di}$ [30]:

$$\left(k_La\right)_{su} = 0.34\left(k_La\right)_{di} \tag{13}$$

In the HTLB, Eq. (13) shows the correlation with its corresponding coefficient and powers as well [7]:

$$k_La_{O_2} = 1.25U_{sG}^{0.38}\cdot U_{sL}^{1.06}\cdot\left(\frac{L}{D}\right)^{-0.69}\cdot\left(1+S\right)^{-0.025} \tag{13}$$

As Eq. (13) shows, the oxygen mass transfer coefficient is more influenced by liquid superficial velocity. Its range of applicability is between 0.01-0.05 m.s^{-1} and 0.12-0.47 m.s^{-1} for superficial gas and liquid

velocities respectively. L/D is between 37-54. Also, S is 0.61 to 1.65. The unit of k_La is time reverse (s^{-1}). Eq. (13) correlated 95% of the data with less than 15% error. This maximum deviation only states in which ranges the measured and calculated data cover each other. The volumetric gas liquid mass transfer coefficient was also determined for methane. Concentration of dissolved methane was measured by methane detector and its volumetric coefficient determined by a simple method addressed previously. Here, methane correlation, is given in Eq. (14) [7]:

$$k_L a_{CH_4} = 0.87 U_{sG}^{0.34} \cdot U_{sL}^{1.05} \cdot \left(\frac{L}{D}\right)^{-0.67} \cdot (1+S)^{-0.023} \quad (14)$$

On average, mass transfer coefficients of oxygen are near to 1.4 folds of that of methane's. Mass transfer coefficient of oxygen with respect to methane has been determined by other researchers and their results are close to the ones obtained in this study (1.12 to 1.43) [54-56]. Also, in other approach, in which mixtures of methane and ethane were examined, an amount of 2.1 has been reported for k_La_{O2}/k_La_{CH4} [57].

The correlation for air k_La in suction part of the VTLB is presented by Eq. (15) [35]:

$$\left(k_L a_{O_2}\right)_{su} = 0.038 U_{sG}^{0.13} \cdot U_{sL}^{0.35} \cdot \left(\frac{H}{D}\right)^{0.13} \cdot (1+S)^{-0.02} \quad (15)$$

Separator volume demonstrates more sensible effect compared to previous correlations. For any combination of gas and liquid flow rates, the measured and calculated k_La values in the suction part agreed on maximum ±14%.

Eq. (16) shows the correlation in discharge side [35]:

$$\left(k_L a_{O_2}\right)_{di} = 0.036 U_{sG}^{0.14} \cdot U_{sL}^{0.30} \cdot \left(\frac{H}{D}\right)^{0.12} \cdot (1+S)^{-0.03} \quad (16)$$

As Eq. (16) shows, the oxygen mass transfer coefficient is more influenced by liquid superficial velocity. Eq. (16) correlated 96% of the data with less than 10% error.

The volumetric gas liquid mass transfer coefficient was also determined for methane. Here, methane correlation in suction side was given in Eq. (17) [35]:

$$\left(k_L a_{CH_4}\right)_{su} = 0.021 U_{sG}^{0.14} \cdot U_{sL}^{0.34} \cdot \left(\frac{H}{D}\right)^{0.12} \cdot (1+S)^{-0.03} \quad (17)$$

On average, mass transfer coefficients of oxygen are equal to 1.85 folds of that of methane's in the suction zone. Mass transfer coefficient of oxygen with respect to methane has been determined by other researchers and their results are close to those obtained in this study (1.43 to 2.1) [54-57]. The range of applicability for Eqs. (15) to (17) are 0.01 to 0.06 $m.s^{-1}$ for superficial gas velocity. The value of H/D is 45 to 67. Also, the ratio of separator volume to discharge side volume is 0.61 to 1.65. Moreover, the liquid flow rate is 0.1 to 0.5 $m.s^{-1}$.

Depending on the gas velocity range the exponent for U_{sG} has the values ranging from 0.13 to 0.60 [7,36,37]. *Chisti et al.* [36], *Fadavi & Chisti* [37] and *Yazdian et al.* [7] determined the exponent of U_{sG} in values of 0.4, 0.54 and 0.38, respectively. It goes without saying that the exponent of U_{sG} in our correlation is in this range. *Chisti et al.* [36] and *Fadavi & Chisti* [37] involved the power input and the volume of the bioreactor to determine the mass transfer coefficient. *Yazdian et al.* [7] reported an exponent of -0.025 for the term (S) in their work. The exponent of (S) in eqs 15 to 17 is next to *Yazdian*'s.

Fig. 15 illustrates the comparison of mass transfer coefficient versus superficial gas velocity for different loop bioreactors. The lowest mass transfer coefficient was achieved in the EALB. In the VTLB, mass transfer coefficient was more than in the forced–liquid HTLB. However, mass transfer coefficients in the HTLB and VTLB were more than in the EALB; because of the increased liquid velocity in the forced-liquid loop bioreactors. Therefore, the experimental results showed that the greatest mass transfer coefficients were obtained significantly in the VTLB. According to experimental outcomes, the forced-liquid circulation (in the VTLB) led to an extension in the mass transfer coefficient about 72% compared to the EALB. However, the forced-liquid flow rates in the HTLB resulted to an extension in values of k_La about 41% compared to the EALB. Due to the presented data, a region (it was shown in gray color in Fig. 15) that was independent on bioreactor type (HTLB and EALB) was explored that occurred in superficial gas velocity that ranged between 0.015 $m.s^{-1}$ to 0.047 $m.s^{-1}$. In that zone mass transfer coefficient was not reliant on bioreactor variety (HTLB and EALB) and changed with variation of operational and design parameters only. The comparison of experimental results for mentioned loop bioreactors (based on correlations) are compared in Table 4 as well.

Table 4: Comparison of mass transfer correlations for different loop bioreactors.

characteristics	correlation	R^2
Gas-induced EALB	$(k_La)_{di} = 0.097U_{sG}^{0.46}\cdot\left(1+\frac{A_r}{A_d}\right)^{-0.63}\cdot(1+S)^{-0.61}\cdot\left(\frac{\upsilon_g}{\upsilon_{N_2}}\right)^{-0.91}\cdot\left(\frac{D_g}{D_{N_2}}\right)^{1.12}$	0.94
	$(k_La)_{su} = 0.34(k_La)_{di}$	0.96
Forced-liquid HTLB	$k_La_{O_2} = 1.25U_{sG}^{0.38}\cdot U_{sL}^{1.06}\cdot\left(\frac{L}{D}\right)^{-0.69}\cdot(1+S)^{-0.025}$	0.95
	$k_La_{CH_4} = 0.87U_{sG}^{0.34}\cdot U_{sL}^{1.05}\cdot\left(\frac{L}{D}\right)^{-0.67}\cdot(1+S)^{-0.023}$	0.95
Forced-liquid VTLB	$(k_La_{O_2})_{su} = 0.038U_{sG}^{0.13}\cdot U_{sL}^{0.35}\cdot\left(\frac{H}{D}\right)^{0.13}\cdot(1+S)^{-0.02}$	0.90
	$(k_La_{O_2})_{di} = 0.036U_{sG}^{0.14}\cdot U_{sL}^{0.30}\cdot\left(\frac{H}{D}\right)^{0.12}\cdot(1+S)^{-0.03}$	0.96
	$(k_La_{CH_4})_{su} = 0.021U_{sG}^{0.14}\cdot U_{sL}^{0.34}\cdot\left(\frac{H}{D}\right)^{0.12}\cdot(1+S)^{-0.03}$	0.90

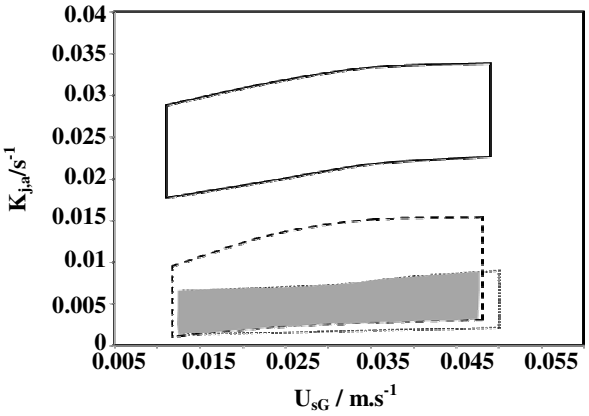

Fig. 15: Comparisons of mass transfer coefficient versus superficial gas velocity for loop bioreactors (forced-liquid VTLB, forced-liquid HTLB and gas-induced EALB): ——forced–liquid VTLB; – – · forced-liquid HTLB; ····· gas-induced EALB.

Comparison of loop bioreactors based on mass transfer efficiency

Mass transfer efficiency E_m is defined as Eq. (17) [5,36]:

$$E_m = \frac{k_La}{e_T} \qquad (18)$$

By multiplying the E_m–value with the steady–state driving force for oxygen transfer (i.e. C* – CL), we can obtain the amount of oxygen transferred per unit of energy supplied. Mass transfer efficiencies for various levels of power input in three loop bioreactors are shown in Fig. 16. For the entire range of liquid flow rates, highest amounts of E_m were obtained only in the VTLB. It is obvious that at low power input (50 to 120 w.m^{-3}); the VTLB is the most efficient bioreactor.[35] However, in the HTLB, highest values were obtained at specific power input values between 30 to 70 w.m^{-3} when the forced circulation rate was ≤0.24 m.s^{-1}. High values of forced circulation rates reduced mass transfer efficiency [36-38]. Also, in the EALB, experimental results show that higher mass transfer efficiency was obtained while U_{sG}≤0.04 m.s^{-1}.

Comparison of loop bioreactors based on biomass production

Due to compare the performance of the EALB, VTLB and HTLB in terms of biomass production, k_La and E_m data, five experiments were designed. In all experiments U_{sG}, U_{sL}, S, A_r/A_d, L/D and H/D were adjusted to the values which resulted the highest mass transfer coefficients in each bioreactor. Fig. 17 demonstrates the scenario of five biomass growth based on the results of optical density at 600 nm for different gas mixtures in the loop bioreactors. All experiments were started by 7 volume percent inoculum of active *Methylomonas* culture

Table 5: Comparison of different loop bioreactors for biomass production in optimum conditions.

characteristics	Oxygen to methane ratio (vol%)	$(k_La)_{O2}$ (s^{-1})	E_m	Optical density (-)	Dry cell weight (g/L)	Doubling time (min)
gas-induced EALB	75 to 25	0.0074	4	0.94	1.02	155
forced-liquid HTLB	50 to 50	0.016	6	1.20	2.45	104
forced-liquid VTLB	60 to 40	0.034	15	3.00	2.97	96

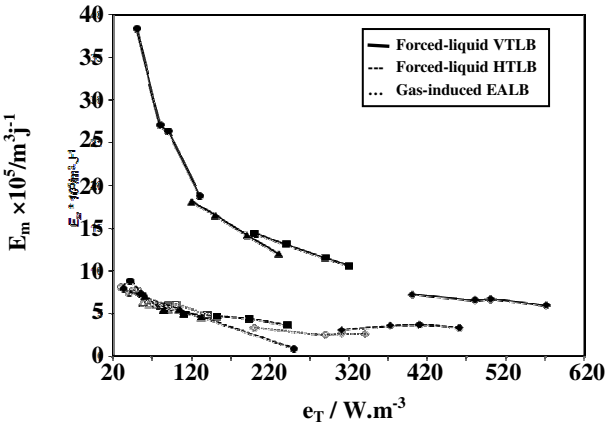

Fig. 16: Comparison of mass transfer efficiency (E_m) in different loop bioreactors.

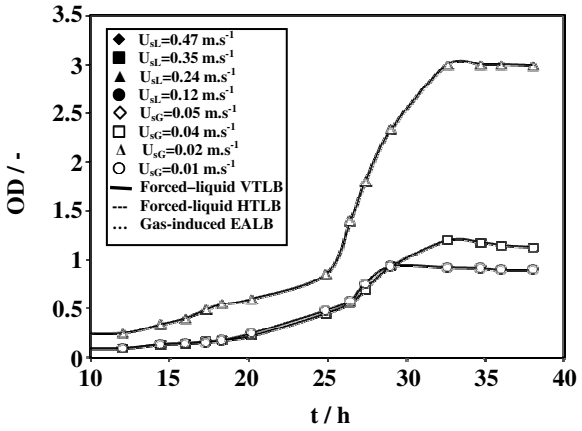

Fig. 17: Optical density of MSB culture versus time at 600 nm for different gas mixtures in the VTLB, HTLB and EALB.

and carried out in triplicate. Fig. 17 and Table 5 show that a gas mixture of 25 vol% methane and 75 vol% oxygen gives the best biomass production in the EALB (maximum optical density: 0.94; doubling time: 155 min). Although 75 vol% methane provides the best k_La (0.0041 s^{-1}), it resulted in the worst biomass growth. Moreover, a gas mixture of 50 vol% air and 50 vol% methane gives the best biomass production (maximum optical density: 1.2; doubling time: 104 min) in the HTLB and a gas mixture of 40 vol% methane and 60 vol% air provides the best biomass production (maximum optical density: 3; doubling time: 96 min) in the VTLB. These explain that in methane fermentation, despite of the greater value of k_La for oxygen, the rate of oxygen transfer may be more critical than that of methane. This fact has been investigated by other studies and presented in other ways [5,58-60].

CONCLUSIONS

For comparison of the performance of different loop bioreactors (EALB, HTLB and VTLB), different specific power input, aeration rates and liquid flow rates were employed to obtain reliable results. Gas-liquid mass transfer was distinguished in the three kinds of loop bioreactors for various combinations of design and operational parameters as well as gas phase properties for production of biomass from natural gas. The results presented in this work indicated the values of mass transfer coefficients and gas hold−ups in the VTLB was higher than those of HTLB and EALB. Moreover, experimental results showed that higher mass transfer efficiency (E_m) for the entire range of liquid flow rates was obtained in the VTLB, as well. The shortest mixing time was achieved in the VTLB. The VTLB, not only affords a forced liquid flow, but also provides a countercurrent contact between gas and liquid flow. The horizontal loop bioreactor circulates the bubbles by the force of pumped liquid too; however, since it makes bubbles flow in horizontal direction, it creates a moderate mixing time. Generally, those that circulate liquid resulted in lesser (better) mixing time. The conventional EALB, in this comparison, demonstrated the poorest mixing time performance. To show the maximum difference, as Fig. 5 shows, the VTLB can perform a mixing time around 30 percent better than EALB. According to mixing time data, a region that was independent on bioreactor type was explored. In that zone, mixing time was not reliant on bioreactor variety

and varies with variation of operational and design parameters, only. In addition, the lowest gas hold-up was achieved in the EALB. The experimental results showed that the biggest gas hold−ups were obtained noticeably in the VTLB; because of the increased liquid velocity in the forced−liquid loop bioreactors. According to experimental outcomes, the forced−liquid circulation (in the VTLB and HTLB) led to an extension in the gas hold−up about 66% compared to the EALB. Due to the presented data, a region that was independent on bioreactor type (HTLB and VTLB) was determined. In that region, gas hold-up was not dependent on bioreactor selection (HTLB and VTLB) and changed with variation of operational and design parameters, only. This scenario, however, holds true for mass transfer coefficients, too. The lowest mass transfer coefficient was achieved in the EALB. In the VTLB, mass transfer coefficient was more than in the forced−liquid HTLB, as well. However, mass transfer coefficients in the HTLB and VTLB were more than in the EALB. Therefore, the greatest mass transfer coefficients were obtained significantly in the VTLB. Based on experimental results, the forced-liquid circulation (in the VTLB) led to an extension in the mass transfer coefficient about 72% compared to the EALB. However, the forced-liquid flow rates in the HTLB resulted to an extension in values of k_La about 41% compared to the EALB. A region that was not dependent on bioreactor kind was considered. In that part, mass transfer coefficients changed only with differences of operational and design factors. This research has been devoted to covering mentioned variables to obtain generally applicable equations for the loop bioreactors design in order to produce biomass from natural gas in optimum conditions. Based on hydrodynamic and mass transfer data, the best biomass production occurred in the forced-liquid VTLB for a gas mixture of 40 vol% methane and 60 vol% air.

Acknowledgment

This investigation was supported by National Iranian Oil Company (NIOC) and National Iranian Gas Company (NIGC).

Notations

A_r/A_d	Riser (discharge) to downcomer (suction) cross sectional area ratio, Dimensionless
Bo	Bodenstein number, Dimensionless
C^*	Saturated oxygen concentration, ppm
C_L	DO concentration, ppm
D_0	Holes size in sparger, mm
D_{di}	Discharge diameter, m
D_g	Diffusion coefficient, $m^2.s^{-1}$
D_{su}	Suction diameter, m
D_s	Separator diameter, m
e_T	Total power input per unit volume, $W.m^{-3}$
g	Gravitational acceleration, $m.s^{-2}$
h_b	Bioreactor height, m
h_s	Liquid level in separator, m
H_d	Downcomer height, m
H_r	Riser height, m
H/D	Vertical length to diameter/ dimensionless
k_La_{CH4}	Volumetric methane mass transfer coefficient, s^{-1}
k_La_{O2}	Volumetric oxygen mass transfer coefficient, s^{-1}
L/D	Horizontal length to diameter, dimensionless
M	Molar mass, $kg.kmol^{-1}$
N	Number of holes in distributor, dimensionless
P_M	Power input due to agitator, W
P_{ts}	Pressure at top section, Pa
Q_L	Volumetric liquid flow rate, $m^3.h^{-1}$
Q_m	Molar gas flow rate, $kmol.s^{-1}$
R	Universal gas constant, $J.kmol^{-1}.K^{-1}$
t	Time, h
U_{sG}	Superficial gas velocity in riser, $m.s^{-1}$
U_{sL}	Superficial liquid velocity, $m.s^{-1}$
v_0	Gas velocity through the sparger hole, $m.s^{-1}$
V_L	Liquid velocity, $m.s^{-1}$

Abbreviations

DO	Dissolved oxygen, ppm
EALB	External airlift loop bioreactor
HTLB	Horizontal tubular loop bioreactor
LP	Liquid pump
MP	Magnetic pump
TLC	Temperature loop controller
VTLB	Vertical tubular loop bioreactor
OD	Optical density, dimensionless

Greek letters

ε	Gas hold-up, dimensionless
ε_{di}	Gas hold-up in discharge, dimensionless
ε_{su}	Gas hold-up in suction, dimensionless

ρ_L	Liquid density, $kg.m^{-3}$
Ω	Efficiency factor
υ_g	Kinematic gas viscosity, Pa.s
υ_{N2}	Kinematic nitrogen viscosity, Pa.s

Received : Jan 5, 2010 ; Accepted : March 1, 2011

REFERENCES

[1] Schüger S., Comparison of Different Loop Bioreactors, *Bioproc. Eng.*, **9**, p. 215 (1993).

[2] Larsen E. B., U-Shape and/or Nozzle U-Loop Fermentor and method of carrying out a Fermentation Process, US. Pat. 6492135B1 (2002).

[3] Blenke H., Loop Reactors, *Adv. Biochem. Eng.*, **13**, p. 121 (1979).

[4] Lars J., Method and Means for the Production of a Microorganism Cell Mass, EP. Pat. 0306466A2 (1989).

[5] Kurt S., Lars J., Henrik E., Method of Fermentation, WO. Pat. 016460A1 (2003).

[6] Chisti Y., "Airlift Bioreactors", Elsevier, London, (1989).

[7] Yazdian F., Shojaosadati S.A., Nosrati M., Mehrnia M.R., Vasheghani-Farahani E., Study of Geometry and Pperational Conditions on Mixing time, Gas Hold up, Mass Transfer, Flow Regime and Biomass Production from Natural Gas in a Horizontal Tubular Loop Bioreactor, *Chem. Eng. Sci.*, **64**, p. 540 (2009).

[8] Koffas M., Odom J.M., Schenzle A., High Growth Methanotrophic Bacterial Strains, WO. Pat. 0220728A2 (2002).

[9] Yazdian F., Hajizadeh S., Shojaosadati S.A., Khalilzadeh R., Jahanshahi M., Nosrati M., Production of Single Cell Protein from Natural Gas: Parameter Optimization and RNA Evaluation, *Iranian J. Biotech.*, **3**, p. 235 (2005).

[10] Yazdian F., Pesaran Hajiabbas M., Shojaosadati S.A., Nosrati M., Mehria M., Vasheghani-Farahani E., Evaluation of Gas Hold-Up and Mixing Time in Loop Bioreactors During Production of SCP from Natural Gas, The Second International Conference on Environmental, Industrial and Applied Microbiology, Seville, Spain (2007).

[11] Whittenbury R., Phillips K.C., Wilkinson J.F., Enrichment, Isolation and Some Properties of Methane Utilizing Bbacteria, *J. Gen. Microbiol.*, **61**, p. 205 (1970).

[12] Dalton H., The Leeuwenhoek Lecture 2000 The Natural and Unnatural History of Methane-Oxidizing Bacteria, Philosophical Transactions of the Royal Society B: *Biological Sciences*, **360**, p. 1207 (2005).

[13] Urmann K., Norina E.S., Schroth M.H., Zeyer J., Methanotrophic Activity in a Diffusive Methane/ Oxygen Counter-Gradient in an Unsaturated Porous Medium, *J. Contam. Hydrol.*, **94**, p. 126 (2005).

[14] Ziegler H., Meister D., Dunn I.J., The Tubular Loop Fermentor: Oxygen Transfer, Growth Kinetics, and Design, *Biotech. Bioeng.*, **XIX**, p. 507 (1977).

[15] Papagianni M., Matty M., Kristiansen B., Design of a Tubular Loop Bioreactor for Scale-Up and Scale-Down of Fermentation Processes, *Biotech. Prog.*, **19**, p. 1498 (2003).

[16] Wen J., Chen Y., Chen D., Jia X., Removal of Ethyl Acetate in Air Streams Using a Gas-Liquid-Solid Three-Phase Flow Airlift Loop Bioreactor, *Biochem. Eng. J.*, **24**, p. 135 (2005).

[17] White E.A., Improvement in or Relating to Fermentation Processes for Converting Methane into Proteinaceous Material, UK. Patent, 1463295 (1977).

[18] Papagianni M., Matty M., Kristiansen B., Citric Acid Production and Morphology of *Aspergillus niger* as Functions of the Mixing Intensity in a Stirred Tank and a Tubular Loop Bioreactor, *Biochem. Eng. J.*, **2**, p. 197 (1998).

[19] Taweel A.M., Yan J., Azizi F., Odedra D., Gomma H.G., Using in-Line Static Mixers to Identify Gas-Liquid Mass Transfer Processes, Chem. Eng. Sci., **60**, p. 6378 (2005).

[20] Sheehan B.T., Johnson M.J., Production of Bacterial Cells from Methane, Appl. Microbiol., **21**, p. 511 (1971).

[21] Lamb S.C., Garver J.C., Batch- and Continuous-Culture Studies of a Methane-Utilizing Mixed Culture, *Biotech. Bioeng.*, **22**, p. 2097 (1980).

[22] Coulson J.M., Richardson J.F., Backhurst J.R., Harker J.H., "Chemical Engineering", Pergamon, Oxford, (1990).

[23] Popovic M., Robinson C.W., Mixing Characteristics of External Loop Airlifts: Non-Newtonian Systems, *Chem. Eng. Sci.*, **45**, p. 1405 (1993).

[24] Rousseau J., Bu'Lock J.D., Mixing Characteristics of A Simple Airlift, *Biotech. Lett.*, **2**, p. 475 (1980).

[25] Gavrilescu M., Tudose R.Z., Mixing Studies in External-Loop Airlift Reactors, *Chem. Eng. J.*, **66**, p. 97 (1997).

[26] Weiland P., Influence of Draft Tube Diameter on Operation Behavior of Airlift Loop Reactors, *Ger. Chem. Eng.*, **7**, p. 374 (1984).

[27] Chisti M.Y., Kasper M., Moo-Young M., Mass Transfer in External Loop Airlift Bioreactors Using Static mixers, *Canadian J. Chem. Eng.*, **68**, p. 45 (1990).

[28] Choi K.H., Han B.H., Lee W.K., Effect of Horizontal Connection Pipe Length on Gas Hold up and Volumetric Oxygen Transfer Coefficient in External Loop Airlift Reactor, *HWAHAK KONGHAK,* **28**, p. 220 (1990).

[29] Petrović D.Lj., Pošarac D., Prediction of Mixing Time in Airlift Reactors, *Chem. Eng. Comm.*, **133**, p. 1 (1995).

[30] Yazdian F., Shojaosadati S.A., Nosrati M., Pesaran HajiAbbas M., Vasheghani-Farahani E., Investigation of Gas Properties, Design, and Operational Parameters on Hydrodynamic Characteristics, Mass Transfer, and Biomass Production from Natural Gas in an External Airlift Loop Bioreactor, *Chem. Eng. Sci.*, **64**, p. 2455 (2009).

[31] Lu X., Ding J., Wang Y., Shi J., Comparison of the Hydrodynamics and Mass Transfer Characteristics of a Modified Square Airlift Reactor with Common Airlift Reactors, *Chem. Eng. Sci.*, **55**, p. 2257 (2000).

[32] Mirón S.A., García C.M.C., Camacho G.F., Grima M.E., Chisti Y., Mixing in Bubble Column and Airlift Reactors, *Chem. Eng. Res. Des.*, **82**, p. 1367 (2004).

[33] Bello R.A., Robinson C.W., Moo-Young M., Liquid Circulation and Mixing Characteristics of Airlift Contactors, *Canadian J. Chem. Eng.*, **62**, p. 573 (1984).

[34] Joshi J.B., Ranade V.V., Gharat S.D., Lele S.S., Sparged Loop Reactors, *Canadian J. Chem. Eng.*, **68**, p. 705 (1990).

[35] Yazdian F., Shojaosadati S.A., Nosrati M., Vasheghani-Farahani E., Study of Hydrodynamic, Mass Transfer, Energy Consumption and Biomass Production from Natural gas in a Forced-Liquid Vertical Tubular Loop Bioreactor, *Biochem. Eng. J.*, **49**, p. 192 (2009).

[36] Chisti M.Y., Jauregui-Haza U.J., Oxygen Transfer and Mixing in Mechanically Agitated Airlift Bioreactors, *Biochem. Eng. J.*, **10**, p. 143 (2002).

[37] Fadavi A., Chisti Y., Gas-Liquid Mass Transfer in a Novel Forced Circulation Loop Reactor, *Chem. Eng. J.*, **112**, p. 73 (2005).

[38] Fadavi A., Chisti Y., Gas Hold Up and Mixing Characteristics of a Novel Forced Circulation Loop Reactor, *Chem. Eng. J.*, **131**, p. 105 (2007).

[39] Papagianni M., Matty M., Kristiansen B., Citric Acid Production and Morphology of *Aspergillus Niger* as Functions of the Mixing Intensity in a Stirred Tank and a Tubular Loop Bioreactor, *Biochem. Eng. J.*, **2**, p. 197 (1998).

[40] Verlaan P., Van E.A.M.M., Tramper J., Van't R.K., Luyben K.Ch.A.M., Estimation of Axial Dispersion in Individual Sections of an Airlift-Loop Reactor, *Chem. Eng. Sci.*, **44**, p. 1139 (1989).

[41] Bello R.A., Robinson C.W., Moo-Young M., Gas Hold-up and Volumetric Mass Transfer Coefficient in Airlift Contactors, *Biotech. Bioeng.*, **27**, p. 369 (1985a).

[42] Chisti M.Y., Halard B., Moo-Young M., Liquid Circulation in Airlift Reactors, *Chem. Eng. Sci.*, **43**, p. 451 (1988).

[43] Kawase Y., Tsujimura M., Yamaguchi T., Gas Hold Up in External Loop Airlift Bioreactors, *Bioproc. Biosys. Eng.*, **12**, p. 21 (1995).

[44] Akita K., Yoshida F., Gas Hold-Up and Volumetric Mass Transfer Coefficient in Bubble Columns, *Ind. Eng. Chem. Proc. Des. Dev.*, **12**, p. 76 (1973).

[45] Schumpe A., Deckwer W.D., Viscous Media in Tower Bioreactor: Hydrodynamic Characteristics and Mass Transfer Properties, *Bioproc. Eng.*, **2**, p. 79 (1987).

[46] Chisti M.Y., Fujimoto K., Moo-Young M., Hydrodynamic and Oxygen Mass Transfer Studies in Bubble Columns and Airlift Bioreactors, Paper 117a presented at AICHE Annual Meeting, Miami Beach (1986).

[47] Bello R.A., Robinson C.W., Moo-Young M., Prediction of the Volumetric Mass Transfer Coefficient in Pneumatic Contactor, *Chem. Eng. Sci.*, **40**, p. 53 (1985b).

[48] Chisti M.Y., Halard B., Moo-Young M., Liquid Circulation in Airlift Reactors, *Chem. Eng. Sci.*, **43**, p. 451 (1988).

[49] Schumpe A., Die Chemische Bestimmung von Phasengrenzflächen in Blasensäulen Bei Uneinheitlichen Blasengrößen, Dr. Thesis, Universität Hannover (1981).

[50] Deckwer W.D, Nguyen-Tien K., Schumpe A., Serpemen Y., Oxygen Mass Transfer into Aerated CMC Solutions in a Bubble Column, *Biotech. Bioeng.*, **24**, p. 461 (1982).

[51] Mohanty K., Dasb D., Biswas M.N., Mass Transfer Characteristics of a Novel Multi-Stage External Loop Airlift Reactor, *Chem. Eng. J.*, **133**, p. 257 (2007).

[52] Nikakhtari H., Hill G.A., Hydrodynamic and Oxygen Mass Transfer in an External Loop Airlift Bioreactor with a Packed Bed, *Biochem. Eng. J.*, **27**, p. 138 (2005).

[53] Choi K.H., Circulation of Gas and Liquid Phases in External Loop Airlift Reactors, *Chem. Eng. Comm.*, **160**, p. 103 (1997).

[54] Sheehan B.T., Johnson M.J., Production of Bacterial Cells from Methane, *Appl. Microbiol.*, **21**, p. 511 (1971).

[55] Lamb S.C., Garver J.C., Batch- a nd Continuous-Culture Studies of a Methane-Utilizing Mixed Culture, *Biotech. Bioeng.*, **22**, p. 2097 (1980).

[56] Yinghao Y., Ramsay J.A., Ramsay B.A., On-Line Estimation of Dissolved Methane Concentration During Methanotrophic Fermentations, *Biotech. Bioeng.*, **95**, p. 788 (2006).

[57] Volesky B., Zajic J.E., Batch Production of Protein from Ethane and Ethane-Methane Mixtures, *Appl. Microbiol.*, **21**, p. 614 (1971).

[58] Vary P.S., Johnson M.J., Cell Yields of Bacteria Grown on Methane, *Appl. Microbiol.*, **15**, p. 1473 (1967).

[59] House A., Place E., Improvement in or Relating to the Fermentation of Methane Utilizing Microorganism, GB. Patent, 1270006 (1972).

[60] Harrison E.F., Doddema H.J., P rocess for the Production of Micro-Organisms, US. Patent 4042458 (1977).

[61] Yazdian F., Shojaosadati S.A., Nosrati M., Malek KH., Mehrnia M.R., On-Line Measurement of Dissolved Methane Concentration During Methane Fermentation in a Loop Bioreactor, *Iran. J. Chem. & Cehm. Eng.,* **28**, p. 85 (2009).